Shichida, Y., Ono, T., Yoshizawa, T., Matsumoto, H., Asato, A. E., Zingoni, J. P., & Liu, R. S. H. (1987) *Biochemistry 26*, 4422–4428.
Smith, S. O., Friedlander, J., Palings, I., Courtin, J., DeGroot, H., Lugtenburg, J., Mathies, R. A., & Griffin, R. G. (1988) *Biophys. J. 53*, 385a.
Wald, G., Brown, P. K., & Smith, P. H. (1955) *J. Gen. Physiol. 38*, 623–681.

Activation Parameters for the Halorhodopsin Photocycle: A Phase Lifetime Spectroscopic Study of the 520- and 640-Nanometer Intermediates†

Donald B. Spencer and T. G. Dewey*
Department of Chemistry, University of Denver, Denver, Colorado 80208
Received August 30, 1989; Revised Manuscript Received November 27, 1989

ABSTRACT: Phase lifetime spectroscopy is used to investigate the kinetics of the 520- and 640-nm intermediates in the halorhodopsin photocycle. These intermediates decay on the millisecond time scale and are strongly implicated in the chloride transport steps. The temperature dependence of the 520 and 640 relaxations was measured for chloride and nitrate buffers at pH 6, 7, and 8 and for iodide buffer at pH 6. The 640 relaxations have small activation energies but large entropy barriers. The two relaxation times observed for the 640 intermediate were interpreted by using a mechanism in which two 640 species exist in equilibrium. The second 640 species is not along the main decay path for the photocycle. A quantitative analysis of the data allowed rate constants and activation parameters to be calculated for the elementary steps of this isomerization process. These parameters are similar for both chloride and nitrate buffers but differ somewhat in iodide. The derived calculated rate constants were consistent with the relaxation times observed for the 520 intermediate. These results indicate that the 520 and two 640 intermediates have very similar free energies as well as similar free energies of activation for the various interconversion processes.

Halorhodopsin (hR),[1] a membrane-bound, retinal protein of *Halobacterium halobium*, functions as a light-driven, inward-directed chloride pump [for a review, see Lanyi (1986a)]. Decay of the initial photoproduct through a series of photocycle intermediates is accompanied by translocation of chloride across the cell membrane. Spectroscopic studies have revealed similarities in the photointermediate absorption maxima and kinetics of the photocycles of hR and bacteriorhodopsin (bR), the light-driven proton pump of *H. halobium* (Zimányi et al., 1989). There is also evidence of structural similarity between the two proteins, which have 28% homology in their amino acid sequences (Blanck & Oesterhelt, 1987). One notable difference in the hR and bR photocycles involves the M_{412} intermediate which corresponds to a deprotonated state of the Schiff base linking retinal to the protein. In bR, the M_{412} intermediate has been implicated in proton transport [cf. Lewis et al. (1974)] while in hR the M-like state appears to be a nonproductive side branch of the main photocycle (Hegemann et al., 1986; Lanyi & Schobert, 1983). These similar proteins which transport very different ions provide an opportunity to identify common features of light-driven ion transport.

The general features of the hR photocycle are outlined in Figure 1. This scheme was mainly derived from previous work (Tittor et al., 1987; Lanyi & Vodyanoy, 1986) but incorporates results from the present study as well. The hR ground state consists of a chloride-dependent equilibrium mixture of the hR_{565} and hR_{578} species. The chloride dissociation constant is estimated to be 10 mM (Tittor et al., 1987). Excitation of the ground state either in the absence of chloride or under saturating chloride results in the formation of the 600-nm absorbing state. The 600-nm intermediate is probably two different species dependent on the path from which it is formed. For it to be one species, chloride must dissociate from hR_{578} in the 5 ps required for formation of hR_{600} (Polland et al., 1985). This would require a dissociation rate constant of 2×10^{11} s^{-1}, which is faster than a diffusion-controlled dissociation (Eigen, 1954; Hemmes et al., 1974). The respective 600 species decay either into the chloride-bound 520 species or into the 640 species. The dissociation constant for chloride in the 520 → 640 equilibrium is estimated at 100 mM (Tittor et al., 1987). This step presumably is the release of the transported ion. Full characterization of these processes is hampered by the lack of sensitive spectroscopic indicators for chloride. The kinetics associated with the 640 species are complex as demonstrated by the observation of several relaxation processes which are very wavelength dependent in the 600–670-nm region (Tittor et al., 1987). In this work, a second 640-nm intermediate is identified as shown in Figure 1. The functional significance of this intermediate remains unclear.

In the present work, phase lifetime spectroscopy is used to measure the relaxation kinetics of the hR_{520} and hR_{640} photointermediates. In previous applications to bR's proton uptake and release kinetics, it was shown that while phase lifetime spectroscopy will give relaxation times similar to flash spectroscopy often the amplitudes of the relaxation processes differ (Sinton & Dewey, 1988). This is a result of the phase mea-

† This research was supported in part by National Science Foundation Grant DMB-8703860.
* Author to whom correspondence should be addressed.

[1] Abbreviations: MOPS, 3-(*N*-morpholino)propanesulfonic acid; MES, 2-(*N*-morpholino)ethanesulfonic acid; Tricine, *N*-[tris(hydroxymethyl)methyl]glycine; DNase, deoxyribonuclease; OG, *n*-octyl β-D-glucopyranoside (octyl glucoside); bR, bacteriorhodopsin; hR, halorhodopsin.

0006-2960/90/0429-3140$02.50/0

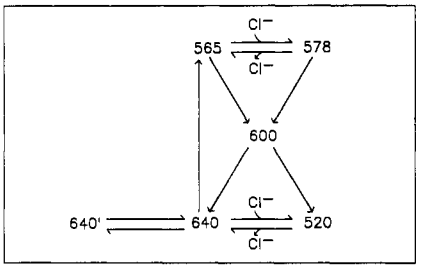

FIGURE 1: Proposed mechanism for light-driven chloride transport by halorhodopsin. The scheme combines features of the mechanisms proposed by Tittor et al. (1987) and Zimányi and Lanyi (1989). The 600 intermediate probably represents two species. Details of the photocycle are described in the text.

surement being made about a photostationary state. It is sometimes possible to observe a relaxation process with one technique which has too small an amplitude to be observed with the other. In the present work, two 640 intermediates are observed. On the basis of this observation, a modification is proposed to the previous hR photocycle mechanisms (Tittor et al., 1987; Lanyi & Vodyanoy, 1986). Activation parameters are determined for the hR 520 and 640 relaxation processes. The activation parameters of several elementary rate constants are also determined by using the proposed mechanism. These results indicate that the 520 and 640 intermediates do not have large differences in their free energy levels but do have significant kinetic barriers. For the 640 intermediates, the activation free energies are dominated by entropy effects.

Materials and Methods

Chemicals. 3-(*N*-Morpholino)propanesulfonic acid (MOPS), MES, Tricine, *n*-octyl β-D-glucopyranoside (octyl glucoside), phenyl-Sepharose CL-4B, and DNase were obtained from Sigma Chemical Co. Bacteriological peptone was from Oxoid Ltd.; Bio-Gel hydroxylapatite was from Bio-Rad Laboratories; Extracti-Gel D was from Pierce Chemical Co.

Protein Purification. Halorhodopsin was purified from bR-deficient *H. halobium* strain OD2 by modification (Hasselbacher et al., 1988) of the procedure of Steiner and Oesterhelt (1983) with the following changes. In the membrane concentration and OG extraction steps, centrifugation was at 120000*g* and 10 °C for 60 min. Pooled purple fractions from the second phenyl-Sepharose column eluant were concentrated to an optical density of 1.0 at 580 nm and then eluted through an Extracti-Gel D column to remove detergent. The sample was then dialyzed against 2 M NaCl/20 mM MES, pH 6.0, buffer. Buffers used were 2 M NaCl, NO_3^-, or I^-, 20 mM MES, pH 6.0, 2 M NaCl or NO_3^-, 20 mM MOPS, pH 7.0, 2 M NaCl or NO_3^-, and 20 mM Tricine, pH 8.0. Buffer changes were accomplished by dialysis of the sample against (3 × 100)-fold excess of the desired buffer.

Phase Lifetime and Absorbance Spectroscopy. Amplitude dispersion data were collected by using the phase lifetime spectrometer (Hasselbacher et al., 1986) interfaced with an IBM-XT computer through a DT2801A data acquisition board (Data Translation) for automated data acquisition. Modulated absorbance amplitudes were measured over a frequency range of 5–500 Hz. A 520- or 500-nm narrow-band interference filter (Oriel Corp., Stratford, CT) was placed before the photomultiplier tube to detect absorbance changes of the hR_{520} intermediate. The hR_{640} intermediate was measured by using two Corning CS 2-64, 666-nm sharp-cut filters (Corning Glass Works, Corning, NY) or a 670-nm narrow-band interference filter (Oriel Corp.) before the phototube and a monochromator setting of 670 nm. This wavelength avoided overlap with the other spectral intermediates. The actinic source driving the photosystem was filtered with a 580-nm narrow-band interference filter (Oriel Corp.). This choice of excitation wavelength minimized photoreaction with the 520 intermediate because of the small spectral overlap with that intermediate. To check for photoreaction with the 640 intermediate, the actinic light intensity was varied by using Oriel neutral density filters (0.5 and 1.0 OD). This provided a change of roughly an order of magnitude in light intensity without changing beam characteristics. All samples were thermostated in a jacketed quartz cell (Precision Cells, Inc.). Absorbance spectra were measured with a Cary 219 spectrophotometer. Chloride titrations were made into a starting volume of hR containing 2 M $NaNO_3$. Lifetimes and amplitudes of the amplitude dispersion curves were obtained from a nonlinear least-squares fit to the amplitude response function as described previously (Sinton & Dewey, 1988).

Results

At pH 6.0 in the high-chloride buffer, a relaxation time of 34 ms was observed for the 520-nm intermediate, and two relaxations of 0.41 and 7.1 ms were observed for the 640-nm species. These results from phase lifetime spectroscopy may be compared with those from flash spectroscopy. Lanyi and co-workers analyze decay curves directly from model simulations (Lanyi & Vodyanoy, 1986; Zimányi & Lanyi, 1989), and relaxation times must be calculated from the rate constants. In these models, the 640 and 520 intermediates have identical biphasic decays. The first study gives relaxation times of 0.4 and 40 ms (Lanyi & Vodyanoy, 1986) while the second study gives 0.3 and 20 ms (Zimányi & Lanyi, 1989). Tittor et al. (1987) observed a single 520 decay of 14 ms. The lifetime of the 640 decay was not directly reported in this work. However, a relaxation process of 5 ms was attributed to 520 → 640 equilibration, and a decay of 12 ms was given for 520 → 578 formation. Thus, there is some variance in the flash data, and this presumably is due to the complexity of the photocycle. It should be noted that for the phase lifetime technique the 640 intermediate theoretically will have an additional relaxation associated with the 520 equilibration. In the absence of chloride, no significant relaxation is observed for the 520 intermediate, and again, two relaxations are seen for the 640 intermediate (0.98 and 7.2 ms). As a check against photoreactions of the 640 intermediates, i.e., two-photon photocycles, the dependence of the relaxation times of these intermediates was measured at different light intensities. It is anticipated that two-photon photocycles will have intensity-dependent relaxation times. In both the chloride and nitrate buffers, no changes in lifetimes were observed when the actinic light intensity was changed by an order of magnitude. Signal to noise considerations prevented the measurement of a more extensive dependence. The chloride dependence of the 520 relaxation time was measured (data not shown), and the dependence is in general agreement with previous observations (Zimányi & Lanyi, 1989).

The temperature dependence of these relaxation processes was measured at pH 6, 7, and 8. Figure 2 shows the temperature dependence of the relaxation times at pH 6 for the high-chloride buffer. Also shown is the temperature dependence of the elementary rate constants derived from these data. The rate constants will be discussed in the next section. Figure 3 shows the temperature dependence of the relaxation times for nitrate and iodide buffers at pH 6. In Table I, the activation parameters are compiled for all the conditions studied. Table II shows the calculated parameters for the rate constants. The activation energy, E_a, and entropy, ΔS^*, were

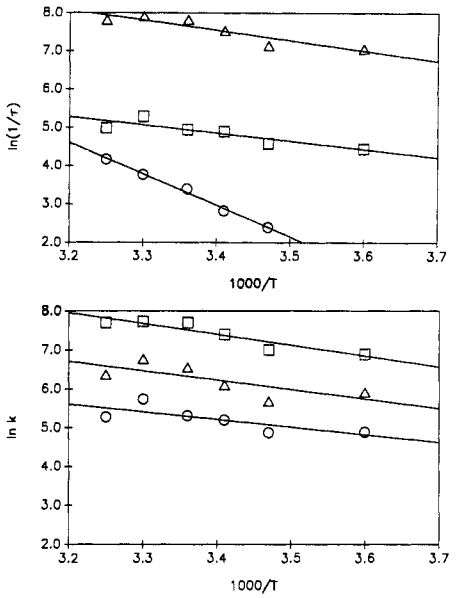

FIGURE 2: (Top) Eyring plot of halorhodopsin 520 and 640 photointermediates. Reciprocal relaxation times were obtained from experiments in 2 M NaCl/20 mM MES, pH 6.0. (△) $640\tau_1$, (□) $640\tau_2$, (○) 520τ. (Bottom) Eyring plot of elementary rate constants derived from the proposed photocycle mechanism using data shown above. (○) k_{-1}, (△) k_1, (□) k_2.

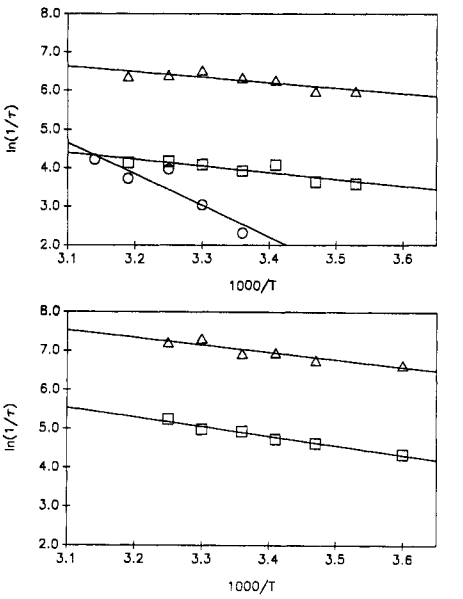

FIGURE 3: Eyring plot of halorhodopsin 520 and 640 photointermediates. Reciprocal relaxation times were obtained from experiments in 2 M NaI/20 mM MES, pH 6.0 (top), and 2 M $NaNO_3$/20 mM MES, pH 6.0 (bottom). (△) $640\tau_1$, (□) $640\tau_2$, (○) 520τ.

Table I: Halorhodopsin Activation Parameters for τ's: pH Dependence in 2 M NaCl, $NaNO_3$, and NaI

	τ_1		τ_2	
	E_a[a]	ΔS	E_a	ΔS
pH 6.0				
640(Cl^-)	4.2 ± 0.9	−37 ± 3	5.3 ± 0.9	−27 ± 3
640-(NO_3^-)	4.9 ± 0.3	−34 ± 1	3.8 ± 0.6	−34 ± 2
640(I^-)	3.5 ± 0.7	−41 ± 2	2.8 ± 0.7	−39 ± 2
520(Cl^-)	16 ± 1	−1.4 ± 2.1		
520(I^-)	17 ± 3	−1.7 ± 11.2		
pH 7.0				
640(Cl^-)	3.3 ± 1.4	−41 ± 5	0.2 ± 1.2	−47 ± 4
640-(NO_3^-)	3.6 ± 6	−40 ± 2	2.6 ± 0.7	−39 ± 2
520(Cl^-)	10 ± 1	−21 ± 2		
pH 8.0				
640(Cl^-)	9.0 ± 1.0	−22 ± 3	6.8 ± 0.8	−24 ± 3
640-(NO_3^-)	8.0 ± 2.0	−26 ± 7	6.0 ± 3.0	−27 ± 10
520(Cl^-)	9.7 ± 0.7	−24 ± 2		

[a] E_a in kilocalories per mole. ΔS in calories per mole per degree kelvin.

determined from a linear least-squares fit to the Eyring equation [cf. Laidler (1965)]:

$$\ln (1/\tau) = \ln (ekT/h) + \Delta S^{\ddagger}/R - E_a/RT \quad (1)$$

where k, h, and R are Boltzmann's, Planck's, and the gas constant, respectively. As can be seen from Table I, the energies of activation for the 640 decay processes are very small. Nevertheless, there is a significant $\Delta G^{\ddagger}$ as a result of a large unfavorable entropy barrier. For the 520 decay process, the energy of activation contributes significantly to the barrier, resulting in free energy changes comparable to those seen in the 640 case. The 520 and 640 decay lifetimes do not show a dramatic dependence on pH from pH 6 to 8, suggesting that this region is far from the pK of any acid–base equilibria vital to chloride transport. Throughout this pH range, the 640 intermediates show uniformly low (<10 kcal/mol) activation energies. When chloride is replaced by iodide, small but significant differences in the 640 kinetics occur. Surprisingly, the 520 kinetics show even less of an effect. In the next section, the interpretation of these results with a specific photocycle mechanism is considered.

Analysis of the Photocycle Mechanism. Initially, the 640 intermediate kinetics in the absence of chloride are considered. This case is simpler than the chloride case because it has been established that the 600 intermediate decays rapidly (0.6 μs) to the 640 intermediate (Tittor et al., 1987). Thus, on the time scale of the phase lifetime measurement, the formation of 640 species can be considered to be instantaneous. The object then was to interpret the two lifetimes in terms of a mechanism for the decay of the 640 intermediate. The data consisted of the

Table II: Halorhodopsin Activation Parameters for k_{-1}, k_1, and k_2: pH Dependence in 2 M NaCl, $NaNO_3$, and NaI

	k_{-1}		k_1		k_2	
	E_a[a]	ΔS	E_a	ΔS	E_a	ΔS
pH 6.0						
Cl^-	3.9 ± 1.3	−37 ± 4	4.8 ± 1.8	−32 ± 6	5.5 ± 0.9	−27 ± 3
NO_3^-	3.5 ± 0.4	−38 ± 1	1.0 ± 0.5	−46 ± 2	4.0 ± 0.9	−34 ± 3
I^-	5.0 ± 1.1	−35 ± 4	5.5 ± 1.0	−32 ± 4	3.5 ± 0.8	−37 ± 3
pH 7.0						
Cl^-	5.7 ± 1.3	−32 ± 4	3.2 ± 0.9	−39 ± 3	0.7 ± 0.6	−46 ± 2
NO_3^-	2.3 ± 0.6	−44 ± 2	−1.5 ± 0.8	−56 ± 3	2.8 ± 0.9	−39 ± 3
pH 8.0						
Cl^-	10 ± 1	−17 ± 4	9.0 ± 1.1	−20 ± 4	5.9 ± 0.8	−28 ± 3
NO_3^-	14 ± 2	−5.5 ± 8.2	13 ± 6	−7 ± 19	11 ± 4	−10 ± 15

[a] E_a in kilocalories per mole. ΔS in calories per mole per degree kelvin.

two lifetimes and the ratio of the amplitudes for the respective processes. A number of mechanisms were considered, and the following one was found to be most consistent with the experimental data:

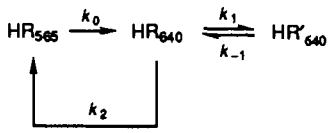

where k_0 is the light-driven step and all the other rate constants are unimolecular. This mechanism shows an isomerization between two 640 species. The second species is not along the path of the decay. The mechanism in which the decay proceeds from the 640′ species did not give physically realistic rate constants. The rate expressions for this mechanism are

$$d[640]/dt = k_0[565] + k_{-1}[640'] - (k_2 + k_1)[640] \quad (2)$$

$$d[640']/dt = k_1[640] - k_{-1}[640'] \quad (3)$$

Using these expressions and the conservation relation, $[HR]_0 = [565] + [640] + [640']$, we can solve the relaxation times and amplitudes. Using the Laplace transform method and amplitude analysis presented previously (Dewey, 1987; Sinton & Dewey, 1988), we obtained the following results:

$$1/\tau_{1,2} = \{(k_2 + 2k_{-1}) \pm \sqrt{k_2^2 + 4k_1k_{-1}}\}/2 \quad (4)$$

where τ_1 is taken to be the plus root and τ_2 is the minus root. The amplitudes observed in the phase lifetime experiments are given by

$$A_1 = \{k_0[HR]_0(k_1 + k_{-1} - 1/\tau_1)\}/\{1/\tau_1(1/\tau_1 - 1/\tau_2)\} \quad (5)$$

$$A_2 = \{k_0[HR]_0(k_1 + k_{-1} - 1/\tau_2)\}/\{1/\tau_2(1/\tau_2 - 1/\tau_1)\} \quad (6)$$

Since three experimental parameters are determined, the three rate constants can be uniquely determined if one assumes that the extinction coefficients for the two 640 states are similar. If the extinction coefficients were not similar, it is anticipated that they would have been distinguishable in previous work employing multichannel transient spectroscopy (Zimányi et al., 1989). The following relationships are used to determine the rate constants:

$$k_1 + k_{-1} = (A_1/A_2 + 1)/(\tau_1 + A_1\tau_2/A_2) \quad (7)$$

$$k_{-1} = [\tau_1 + \tau_2 - \tau_1\tau_2(k_1 + k_{-1})]^{-1} \quad (8)$$

$$1/\tau_1 + 1/\tau_2 = k_2 + 2k_{-1} \quad (9)$$

As a sample calculation at pH 7, 25 °C, in the NO_3^- buffer, the 640 relaxation process has $\tau_1 = 1.9$ ms, $\tau_2 = 15.4$ ms, and $A_1/A_2 = 0.32$, resulting in $k_1 = 109$ s^{-1}, $k_{-1} = 86$ s^{-1}, and $k_2 = 418$ s^{-1}. The rate constants were calculated at each temperature, and the corresponding Eyring plots were constructed. Linear plots were obtained over the entire temperature range at pH 6, 7, and 8. Eyring plots over this limited temperature range (0–40 °C) are expected to be linear. Under a given set of experimental conditions, linearity indicates the consistency of the analysis. It certainly does not prove the mechanism. Small but significant changes occur in the activation parameters with different anions and pH conditions. The results from these calculations are shown in Table II where the activation parameters for the individual rate constants are displayed.

In the presence of chloride, it was found that the 640 intermediate decay parameters did not show large changes. A priori, one could not assume that the above analysis would be appropriate because the decay of the 520 species into the 640 species is not as fast as 600 to 640 in chloride-free solutions. Tittor et al. (1987) estimate this 520 decay process to be 3300 s^{-1} while values of 210 s^{-1} (Lanyi & Vodyanoy, 1986) and 160 s^{-1} (Zimányi & Lanyi, 1989) were previously reported. Additionally in this work, slow 520 decays of approximately 30 ms were observed. Surprisingly, when the above mechanism is used to analyze the chloride-free results, very similar rate constants are obtained. For example, at pH 7, 25 °C, in chloride buffer, $k_1 = 185$ s^{-1}, $k_{-1} = 91$ s^{-1}, and $k_2 = 587$ s^{-1}. The Eyring plots for chloride buffer at pH 6 are shown for the individual rate constants in Figure 2. Activation parameters for all conditions are given in Table II. Again, there is internal consistency. The activation parameters do not differ significantly for the Cl^- and NO_3^- buffers. The I^- does show significant differences.

The lack of a large chloride dependence on the 640 intermediate rate constants can be reconciled by considering the following mechanism for the high-chloride case:

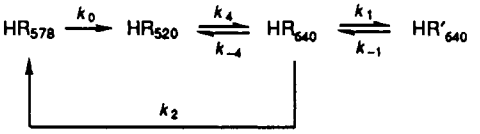

where k_0 is again the light-driven step, and all rate constants are unimolecular except k_{-4} which is bimolecular. The release of chloride has not been explicitly shown in the 520 → 640 step. The complete solution of this mechanism is extremely complex, and the parameters cannot be uniquely determined from the data. The general outlines of its behavior are described here. For phase lifetime spectroscopy, the 640 species will have five relaxation times. Three of these will be associated with the 520 equilibrium. Since a correspondence is not observed with the 520 decay, it is assumed that these processes do not have large amplitudes associated with them. The remaining two lifetimes are given by

$$1/\tau_{3,4} = \{(k_4 + k_1 + k_{-1} + k_2) \pm \sqrt{(k_4 + k_1 + k_{-1} + k_2)^2 - 4k_{-1}k_2}\}/2 \quad (10)$$

Note that eq 10 is quite different in form from eq 4. For pH 6 at 25 °C, the 640 decays are 0.3 and 7.1 ms. If the rate constants obtained from the previous mechanism (eq 5–7) are used along with those determined independently by Zimányi and Lanyi (1989), one has $k_1 = 202$ s^{-1}, $k_{-1} = 699$ s^{-1}, $k_2 = 2205$ s^{-1}, $k_4 = 160$ s^{-1}, and $k_{-4} = 1000$ M^{-1} s^{-1}. Substitution of these values into eq 10 gives relaxation times of 0.5 and 7.1 ms, in excellent agreement with the experimental results. Thus, the two mechanisms are consistent with each other under this specific set of conditions. An additional check is to calculate the relaxation time for the 520 intermediate decay. This decay will have three relaxation times associated with it. The values are the reciprocal roots, λ, of the following cubic equation:

$$(1/\tau_3 - \lambda)(1/\tau_4 - \lambda)(k_1 - \lambda) - k_{-1}k_1(k_{-2} - \lambda) = 0 \quad (11)$$

Equation 11 was solved numerically and gave relaxation times of 40, 3.5, and 0.5 ms. The relaxation time observed in the phase experiment was 33 ms. Again, good correlation with the slow relaxation time is observed. To rigorously test this mechanism, it should be demonstrated that the amplitudes associated with the other two relaxation times are small. Unfortunately, these amplitudes are complex functions of the rate constants and the steady-state concentrations of the intermediates. These arguments do suggest that the two mechanisms considered are not incompatible under these sets

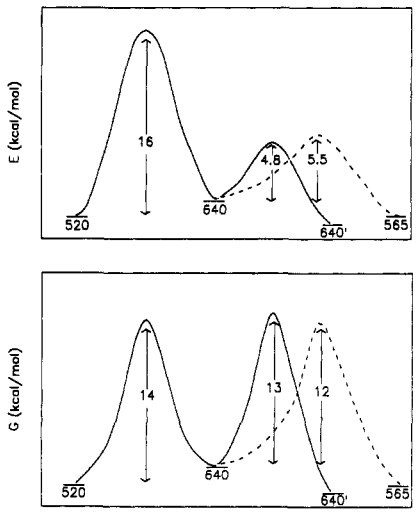

FIGURE 4: Potential energy diagrams for the halorhodopsin photocycle from hR_{520} to hR_{565} based on the mechanism discussed in the text. The ordinate represents energy in kilocalories per mole, and the abscissa represents idealized reaction coordinate. (Top) Peaks represent activation energies. (Bottom) Peaks represent free energies of activation. Relative free energies of intermediates are shown roughly to scale with the exception of the 565 intermediate for which this information is unavailable. Differences in the two plots are due to entropy contributions.

of rate constants. Thus, the rise of the 640 species does not necessarily have to be very rapid for the first mechanism to hold. Conversely, the observed relaxation time associated with the 520 species can be slow even though the 520 precedes the 640 decay. These results are a direct consequence of the complexity of the normal modes associated with relaxation from multiple equilibria.

Discussion

In this work, the existence of a second 640 intermediate in the halorhodopsin photocycle was observed. The kinetic data were found to be consistent with a mechanism in which this second intermediate is an isomerization that is not along the main path of the decay. Mechanisms containing isomeric intermediates are prevalent in the analysis of the bR photocycle [cf. Sinton and Dewey (1988), Birge et al. (1989), and Korenstein et al. (1978)]. As this intermediate is off of the main decay pathway, the functional significance of it is unclear. The second 640 nm intermediate could represent a "back reaction" without chloride to the retinal configuration of the 520 state. The calculated potential barriers for retinal bond rotation in the absence of chloride are not prohibitive (Oesterhelt et al., 1986). Mechanisms consisting of parallel pathways have been proposed for bacteriorhodopsin [cf. Sinton and Dewey (1988) and Birge et al. (1989)]. While such mechanisms cannot be ruled out for halorhodopsin, it would be highly fortuitous for the 520 intermediate to decay along parallel pathways with one relaxation time. Oesterhelt et al. (1986) have proposed a photocycle mechanism in which two 520 isomers exist. In this mechanism, a chloride-bound 520 state with a 13-*cis*,14*s*-*cis*-retinal decays to a 13-*cis*,14*s*-*trans*-retinal state. No kinetic evidence for two 520 intermediates exists at this time. The 13-*cis*,14*s*-*trans*-retinal then releases chloride and forms an *all-trans*-retinal state which absorbs at 640 nm. The single 640 intermediate in Oesterhelt's mechanism can exhibit a biphasic decay as a result of equilibration with the 520 state. However, the lifetimes of at least one of these decays would be expected to be highly dependent on chloride. This is also not observed in the present work. Spectroscopic evidence in bacteriorhodopsin argues against the existence of a 13-cis, 14s-cis species (Fodor et al., 1988; Birge et al., 1989).

In the preceding section, it was argued that the isomerization of the 640 species was uncoupled from the 520 equilibrium under a variety of conditions. These experiments were also performed with iodide replacing chloride. The hope was to slow steps in the mechanism so as to enhance the amplitudes of previously unobserved intermediates. However, no new intermediates were observed. There was a slight enhancement of the 640 amplitudes. The kinetic parameters for the 640 isomerization differ somewhat in iodide as compared with chloride and nitrate. This suggests that in the iodide case the 520 → 640 equilibrium is not completely uncoupled from the 640 isomerization equilibrium.

A simple schematic of the free energy relationships between various intermediates is shown in Figure 4. The activation energies are also displayed in this diagram. This allows the relative contributions of enthalpy and entropy terms to be easily visualized. The 520 → 640 levels were determined by using the data of Zimányi and Lanyi (1989). As can be seen, at this stage of the photocycle, there are not large differences in free energies between intermediates. However, significant kinetic barriers exist for these interconversions. This is reminiscent of free energy diagrams for intermediates in enzyme catalysis (Albery & Knowles, 1976; Knowles, 1987). The optimization of enzymatic processes requires that intermediates interconvert with comparable energy levels. Similar factors may be operative in the optimization of ion-transporting photosystems. Photosystems are of course different from enzymes in that initially there is an enormous input of energy from the photon. There is in fact usually much more energy than the coupled process needs and much of it is lost to thermal relaxation. It is of interest that at this point in the photocycle (520 species onward), there is not a steep downward cascade in the energy levels of the intermediates. This is also the point in the photocycle where the system is primed to released the transported ion. Presumably, most of the photon's energy is spent in the "priming" process, and the ion release steps are accomplished by conformational rearrangements between energetically comparable species. This is consistent with the large entropy barriers observed for some of these interconversions.

Acknowledgments

We thank Dr. Carol Hasselbacher for technical advice in the preparative work and Mark Kurzmack and Tom Hunt for assistance in programming the computer-assisted data acquisition.

References

Albery, W. J., & Knowles, J. (1976) *Biochemistry 15*, 5631–5640.

Birge, R. R., Copper, T. M., Lawrence, A. F., Masthay, M. B., Vasilakis, C., Zhang, C.-F., & Zidovetzki, R. (1989) *J. Am. Chem. Soc. 111*, 4063–4074.

Blanck, A., & Oesterhelt, D. (1987) *EMBO J. 6*, 265–273.

Dewey, T. G. (1987) *Biophys. J. 51*, 809–815.

Eigen, M. (1954) *Z. Phys. Chem. (Frankfurt) 1*, 176.

Fodor, S. P. A., Ames, J. B., Gebhard, R., van den Berg, E. M. M., Stoeckenius, W., Lugtenburg, J., & Mathies, R. A. (1988) *Biochemistry 27*, 7097–7101.

Hasselbacher, C. A., Preuss, D. K., & Dewey, T. G. (1986) *Biochemistry 25*, 668–676.

Hasselbacher, C. A., Spudich, J. L., & Dewey, T. G. (1988) *Biochemistry 27*, 2540–2546.

Hegemann, P., Oesterhelt, D., & Steiner, M. (1986) *EMBO J. 4*, 2347–2350.

Hemmes, P. R., Oppenheimer, L., & Jordan, F. (1974) *J. Am. Chem. Soc. 96*, 6023-6026.
Knowles, J. R. (1987) *Science 236*, 1252-1258.
Korenstein, R., Hess, B., & Kuschmitz, D. (1978) *FEBS Lett. 93*, 266-270.
Laidler, K. J. (1965) *Chemical Kinetics*, 2nd ed., pp 88-90, McGraw-Hill, New York.
Lanyi, J. K. (1986a) *Annu. Rev. Biophys. Biophys. Chem. 15*, 11-28.
Lanyi, J. K. (1986b) *Biochemistry 25*, 6706-6711.
Lanyi, J. K., & Schobert, B. (1983) *Biochemistry 22*, 2763-2769.
Lanyi, J. K., & Vodyanoy, V. (1986) *Biochemistry 25*, 1465-1470.
Lewis, A., Spoonhower, J., Bogomolni, R. A., Lozier, R., & Stoeckenius, W. (1974) *Proc. Natl. Acad. Sci. U.S.A. 71*, 4462-4466.
Oesterhelt, D., Hegemann, P., Tavan, P., & Schulten, K. (1986) *Eur. Biophys. J. 14*, 123-129.
Sinton, M. H., & Dewey, T. G. (1988) *Biophys. J. 53*, 153-162.
Steiner, M., & Oesterhelt, D. (1983) *EMBO J. 2*, 1379-1385.
Stoeckenius, W. (1974) *Proc. Natl. Acad. Sci. U.S.A. 71*, 4462-4466.
Tittor, J., Oesterhelt, D., Maurer, R., Desel, H., & Uhl, R. (1987) *Biophys. J. 52*, 999-1006.
Zimányi, L., & Lanyi, J. K. (1989) *Biochemistry 28*, 5172-5178.
Zimányi, L., Keszthelyi, L., & Lanyi, J. K. (1989) *Biochemistry 28*, 5165-5172.

Carboxy-Terminal Sequencing: Formation and Hydrolysis of C-Terminal Peptidylthiohydantoins†

Jerome M. Bailey and John E. Shively*
Division of Immunology, Beckman Research Institute of the City of Hope, 1450 East Duarte Road, Duarte, California 91010
Received June 30, 1989; Revised Manuscript Received October 23, 1989

ABSTRACT: Proteins and peptides can be sequenced from the carboxy terminus with isothiocyanate reagents to produce amino acid thiohydantoin derivatives. Previous studies in our laboratory indicated that the use of trimethylsilyl isothiocyanate (TMS-ITC) as a coupling reagent significantly improved the yields and reaction conditions and reduced the number of complicating side products [Hawke et al. (1987) *Anal. Biochem. 166*, 298]. The present study further explores the conditions for formation of the peptidylthiohydantoins by TMS-ITC and examines the cleavage of these peptidylthiohydantoin derivatives into a shortened peptide and thiohydantoin amino acid derivative. Schizophrenia-related peptide (Thr-Val-Leu) was used as a model peptide and was treated with acetic anhydride and TMS-ITC at 50 °C for 30 min, and the peptidylthiohydantoin derivatives were isolated by reverse-phase HPLC and characterized by FAB-MS. The purified derivatives were subjected to a variety of cleavage conditions, and rate constants for hydrolysis were determined. Hydrolysis with acetohydroxamate as reported originally by Stark [(1968) *Biochemistry 7*, 1796] was found to give excellent cleavage of the terminal thiohydantoin amino acid, but also led to the formation of stable hydroxamate esters of the shortened peptide which are poorly suited for subsequent rounds of degradation. Hydrolysis with 2% aqueous triethylamine under mild conditions (1-5 min at 50 °C) was found to be more suitable for carboxy-terminal sequence analysis by the thiocyanate method. The shortened peptide, which could be isolated and subjected to a second round of degradation, and the released thiohydantoin amino acid are formed in good yield (90-100%). Several other small peptides containing 15 different C-terminal amino acid side chains were also investigated in order to examine any interfering reactions that might occur when these side chains are encountered in a stepwise degradation using the thiocyanate chemistry. Quantitative yields of peptidylthiohydantoins were obtained for all the amino acids examined with the following exceptions: low yields were obtained for C-terminal Glu or Thr, and no peptidylthiohydantoins were obtained for C-terminal Pro or Asp. Asparagine was found to form cyclic imides (64%) at the penultimate position (C-2) during hydrolysis of the peptidylthiohydantoins by 2% aqueous triethylamine. Cleavage of C-terminal Asn under these conditions led to the formation of the expected shortened peptide (69%), but also to the formation of a shortened peptide (31%) with a C-terminal amide. Problems with Glu and Thr could be solved by minimizing the reaction time with acetic anhydride. Addition of a nucleophile prior to the coupling reaction was used to allow partial degradation of C-terminal Asp. Under a variety of conditions, no peptidylthiohydantoins were formed when Pro was at the C-terminus. Although at this point Pro remains a problem, the combined procedure of reaction with TMS-ITC and hydrolysis with 2% aqueous triethylamine appears suitable for adaptation to a solid-phase extended degradation of peptides and proteins.

The development of methods for the sequential degradation of proteins and peptides from the carboxy terminus is a goal of this laboratory and has been the objective of several studies [for review see Ward (1986) and Rangarajan (1988)]. Such a method would complement existing N-terminal degradations based on the Edman chemistry (Edman, 1950). The most widely studied method and probably the most attractive be-

† This work was supported in part by NSF Grant BBS-8804189.
* To whom correspondence should be addressed.

0006-2960/90/0429-3145$02.50/0